Physica Scripta. Vol. 65, 252–256, 2002

# Survey of Neon and Argon Emission Between 3800 Å and 6000 Å in the EBIT-II Electron Beam Ion Trap

H. Chen[1], P. Beiersdorfer[1], C. L. Harris[2], and S. B. Utter[1]

[1]Department of Physics, Lawrence Livermore National Laboratory, Livermore, CA 94551, USA
[2]Department of Physics, University of Nevada Reno, Reno, NV 89557, USA

*Received February 14, 2001; revised version received July 2, 2001; accepted September 19, 2001*

PACS Ref: 52.25.RV, 52.70.KZ, 32.30.Jc

**Abstract**

Using the low-energy electron beam ion trap EBIT-II at the Lawrence Livermore National Laboratory, we surveyed neon and argon spectra throughout the wavelength range from 3800 to 6000 Å employing a prism spectrograph and a scientific-grade CCD camera. By varying the electron beam energy, spectra from singly ionized to highly ionized neon and argon ions were recorded. In total, about 130 lines were observed from ions in low charge states. About half of the lines have not been reported before. From high charge state ions, several lines of forbidden transitions were observed, among which are the prominent M1 transitions from Ar XIV at 4412 Å and Ar X at 5534 Å.

## 1. Introduction

Optical spectra are important for the diagnostics of laboratory and stellar plasmas. For example, in the edge and divertor regions of tokamak and stellarator fusion plasmas, many low charge-state ions are present because of the relatively low temperature (50–1000 eV in a large tokamak plasma) compared to the plasma central region. Optical emission is abundant from these low charge state ions and is of crucial importance for determining the local plasma conditions. Although most of the resonance lines of highly charged ions are in the X-ray region, some forbidden lines of these ions appear in the optical region. A number of forbidden transitions have already been observed from stellar plasmas and from tokamak plasmas, (see for example, [1–5]).

Optical transitions offer excellent opportunities for the diagnostics of laboratory plasma given state-of-the-art optical instruments that may include light fiber optics, laser tagging, and solid-state optical elements. Spectral information on noble gases, such as neon and argon, is of particular interest in fusion plasmas following the development of radiative cooling scenarios in which impurities such as neon, argon and krypton are deliberately introduced into the edge and divertor plasma. For astrophysics, ground- based optical detection is feasible because of the low absorption in the visible range by the interstellar and atmospheric matter. This is a big advantage over costly, necessarily space-based, UV and X-ray observations. Ions of neon and argon also play important roles in the study of gaseous nebulae and stars [6].

Spectra of neutral and singly ionized neon and argon have been measured previously using light sources such as a hollow-cathode discharge tube [7,8]. Also, visible spectra of highly charged neon and argon including high $n$, $l$-transitions have been investigated using the beam-foil technique [9,10]. Still, the atomic data for optical transitions, especially for ions with charges higher than $q = 2+$, are grossly incomplete. The line identification in these ions is a daunting task. This is because of the complexity: there are a great number of lines present and many lines are blended. Moreover, different plasmas feature different plasma densities and temperatures and in steady or transient states. Hence they generate different sets of emission lines. In order to make progress, we need as much experimental data as possible.

Electron beam ion traps are an ideal source for the spectral measurement of lines relevant to laboratory and stellar plasma, as they provide ions in all charge states found in laboratory and astrophysical plasmas, and at particle densities that are comparable to those in a laboratory fusion plasma or stellar atmospheres [11]. Previous optical studies of noble gas elements on electron beam ion traps include a number of magnetic dipole transition measurements of xenon [12], krypton [13–18] and the transition rates of forbidden transitions of argon and krypton [19–22].

In this paper we present optical observation of electron beam-excited plasmas at low particle densities and known electron beam energies. Very many features were found. Many of them could be identified and many not. Complete modeling of such spectral emission is still not possible. However, our measurements provide the shape of the spectral emission for well-defined plasma conditions (steady states, known beam energy, limited ion charge states and low density). These plasma conditions are much simpler and better defined than those in more complex sources such as tokamak fusion plasmas and astrophysical plasmas where multiple temperatures and densities are present, in principle simplifying the spectral modeling task. We provide broad-band coverage with moderate resolution spectrograph and thus a survey and spectral inventory useful for judging the emission from low-density plasmas. This work also defines a scope for further spectral studies.

In the following, we describe the experimental set-up and the operating parameters, followed by descriptions of the system calibration and data analysis as well as of the techniques we used to identify spectral lines. The data are presented in Section 3.

## 2. Experiment

Our measurements were performed using the electron beam ion trap EBIT-II [23] at the Lawrence Livermore National Laboratory. The electron beam energy in EBIT-II is limited to values below 35 keV, but this is ample for the production

of all the ion species of present interest. The experiment aimed for survey spectra, and for this purpose preference was given to wavelength coverage over spectral resolution and linearity of the calibration curve. For its well-known advantage of broadband wavelength coverage, we used a Steinheil prism spectrometer equipped with 10-cm diameter $f/4$ lenses for high light collection efficiency. The arrangement of the spectrometer relative to the ion source is illustrated in Fig. 1. The line-of-sight of the spectrometer points directly into the trap region, where the monoenergetic electron beam, confined by a 3 Tesla magnetic field that is produced by super-conducting coils has a diameter of about 60 $\mu$m [24]. Since excitation only takes place inside the electron-beam volume, and most of the spontaneous radiative decays occur in the same volume, the light source was studied without an entrance slit.

The noble gases were injected into the trap using a differentially pumped gas injector. The injection gave an ion density of about $10^8$ cm$^{-3}$ in the trap where the pressure is less than $10^{-10}$ mbar.

Spectra were recorded using a cryogenically cooled scientific-grade CCD camera (manufactured by Photometrics, with a Tektronix chip TK1024). The camera has $1024\times1024$ pixels and $24\,\mu\text{m}\times24\,\mu\text{m}$ pixel size. During the data acquisition, CCD pixels were binned in the non-dispersion direction to 256 data points in order to enhance the signal-to-noise ratio and to reduce the signal readout time. The exposure time for each spectrum was 20 min, producing reasonably intense spectra without severe accumulation of background signal. The background signal also contained spikes resulting from cosmic rays striking the CCD. Fortunately, after data acquisition, these spikes could be removed by using appropriate software, since they tended to be localized in a few pixels and are very intense. There were several sources of stray light in the drift tube including the ion gauge and the electron gun. Care was taken to reduce these as much as possible, for example, by closing off parts of unused instrumentation and turning off all but the essential pressure gauges.

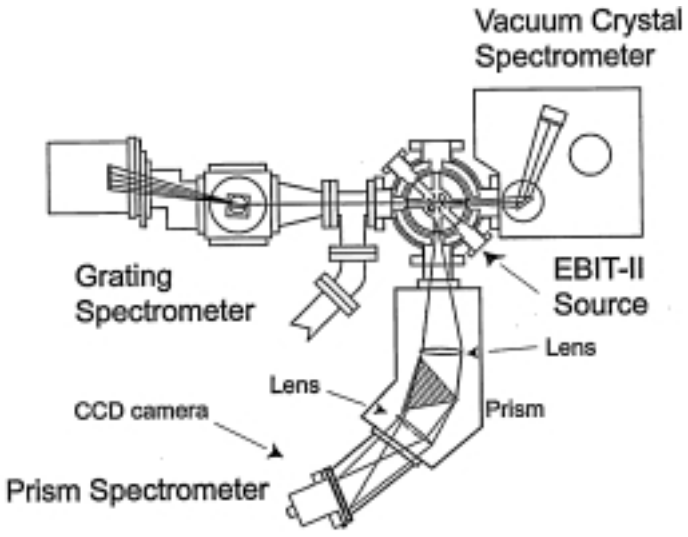


*Fig. 1.* Schematic view of the experimental set up. The position of the prism spectrometer is shown relative to the EBIT-II source, to which also an EUV and an X-ray spectrometer are attached. All these spectrometers use the narrow electron beam excitation zone instead of a physical entrance slit. (Not to scale).

The ionization potential of a elementary species increases with the charge state. Thus the electron beam energy determines the highest charge state present in the trap. In order to identify spectra from individual ionization states, the beam energy was stepped up in small increments so that each energy increase corresponded to the adding of one charge state at the top of the range. A step size of 10 to 20 eV was selected for observing the low charge states, and of 50–100 eV for the higher charge states. In order to record visible emission from low ionization stages, we started with an electron beam energy as low as 150 eV. This minimum energy still ensured the production of a stable and well-confined electron beam. At an electron beam energy of 150 eV, the injected neutral atoms can be ionized up to charge state $q = 6+$. Consequently, we cannot establish individual charge states for low-charge ions. However, one can reduce the charge state range by running the drift tube voltages of the actual trap in the ''inverted-trap mode''. In this mode, the differences of the drift tube voltages are reversed, and thus the potential barrier from the voltage applied to the top drift tube is removed. Ions are then not confined along the trap axis and can escape, and are even accelerated away from the trap. Stepwise ionization by multiple electron-ion collisions consequently is massively reduced. Photons observed are emitted by those atoms from the gas injector that pass through the 60 $\mu$m diameter electron beam. It takes about 0.2 $\mu$s for argon atoms, for example, to cross the beam at thermal energies. During this time, about 20% of the atoms will be ionized once, and 4% may be ionized twice, given an electron energy of 500 eV and an electron density of $10^{12}$ cm$^{-3}$. Double or triple ionization is also possible under single-collision conditions, if inner-shell ionization occurs. Obviously, in the inverted-trap mode, most atoms from the gas injection will remain neutral, and a fraction will be at most a few times ionized before leaving the interaction area. We estimate the highest charge states produced by the inverted trap mode to be less than $q = 5+$. This mode of operation has been used for the *in situ* calibration given that high precision data are available for low charge states elements from standard data bases [25–27].

The calibration of the spectrometer was performed using well-known lines from nitrogen (using molecular nitrogen injection) as well as lines from low charge state ions of neon, argon and krypton. The measured nitrogen spectrum is shown in Fig. 2. It was recorded at an electron beam energy of 1000 eV. Most of the spectral lines have been identified to originate from $q = 0+$ to $q = 2+$ ions. The same spectrometer set-up position was maintained during the measurements. However, shifts of up to 2 pixels (about 50 $\mu$m) occurred on the spectrograph position over the period of a few days, probably caused by mechanical vibrations of surrounding equipment. In order to account for this shift, additional strong lines, for example, carbon (C III at 4647.42 Å), argon (Ar II at 4348.064), and nitrogen (N III at 3998.63 Å), provided an *in situ* wavelength cross-calibration.

Given the demagnification of the optical system, (by a factor of 0.64,) the effective slit width was 38 $\mu$m, which is equivalent to 1.6 pixels. With a typical setting of the prism

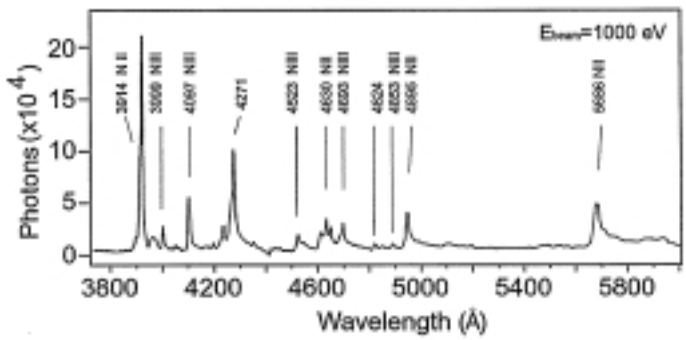


*Fig. 2* Spectrum of nitrogen recorded at an electron beam energy of 1000 eV using the inverted-trap mode. The spectrum was used for the wavelength calibration of the spectrometer. The wavelengths given are from references [25–27].

spectrograph, the full-width-half-maximum (FWHM) line width of an observed line was about 4 pixels, indicating that the instrumental resolution was worse than that given by the source width. The wavelength dispersion of the prism is very non-linear: at 4000 Å it is about 1.28 Å/pixel, and it increases up to 4.80 Å/pixel at 5500 Å. The errors in the wavelength determination are mainly due to the uncertainties resulting from the calibration. The statistical error of the Gaussian line shape fit of each spectrum by comparison is small and typically ranges from 0.01 Å to 0.7 Å., except for several weak lines whose fitting error was as high as a few Ångströms. On average, the accuracy of our wavelength determination ranges from ±6 Å at wavelengths below 4500 Å, and drops to ±16 Å at about 5500 Å.

## 3. Data analysis and results

The emission of the residual background ions and of the stray light signal were recorded each time after taking a spectrum, with exactly the same conditions except for the gas injection being switched off. The background spectrum was then subtracted from the measured gas ion spectrum. However, because the injected ions change the residual ion population, it is difficult to take out the background emission exactly. For example, the C III (4647 Å) line has a higher intensity in the background spectrum than in spectra with gas injection. The line therefore appears with a slightly negative value in background-subtracted spectra, as is visible from Fig. 3 to Fig. 7.

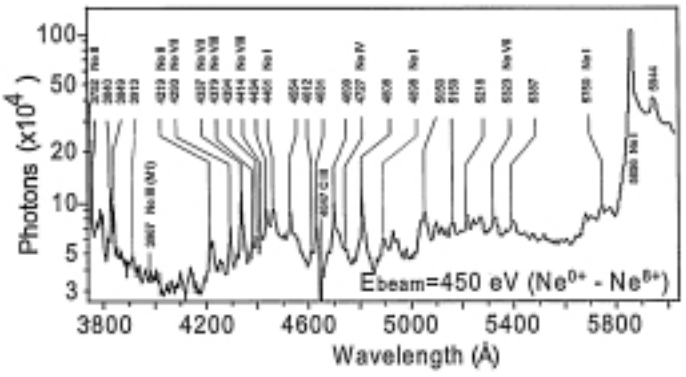


*Fig. 3.* Spectrum of neon recorded at an electron-beam energy of 450 eV. The most prominent lines are given with approximate wavelengths. Ion charge states contributing to this spectrum are $Ne^{0+}$ $Ne^{8+}$.

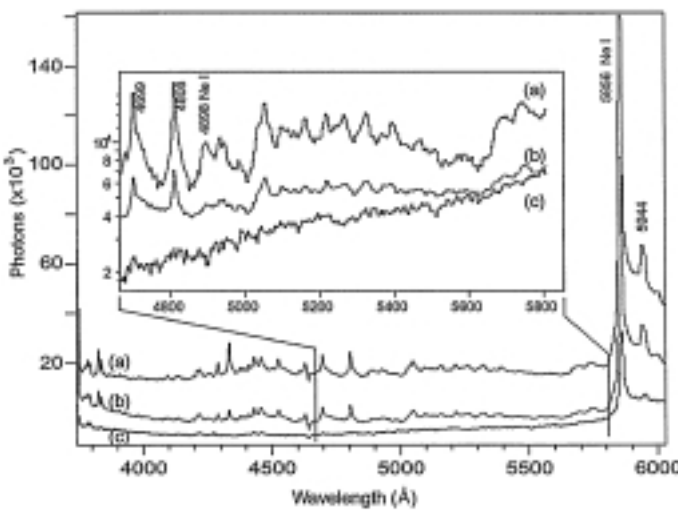


*Fig. 4.* Spectra of neon recorded at three electron beam energies: (a) 170 eV, (b) 250 eV, and (c) 310 eV. The insert shows a section of the spectra on a large scale. The range of ion charge states of each spectrum is (a) $Ne^{0+}$–$Ne^{6+}$, (b) $Ne^{0+}$–$Ne^{8+}$, and (c) $Ne^{0+}$–$Ne^{8+}$.

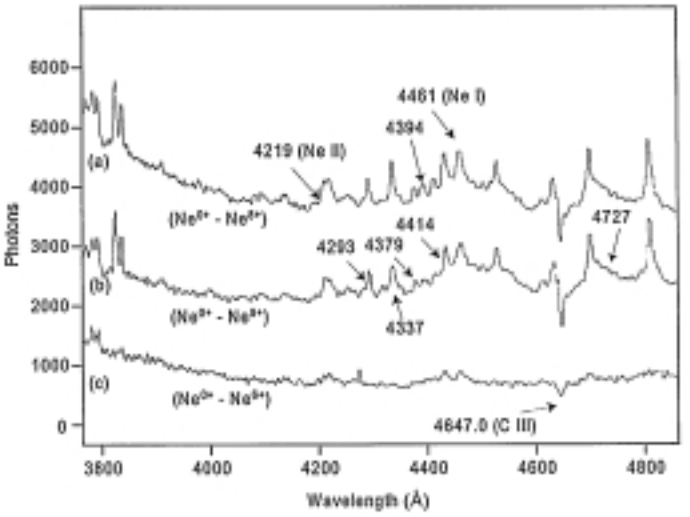


*Fig. 5.* Spectra of neon recorded at three electron beam energies: (a) 170 eV, (b) 250 eV, and (c) 310 eV. The range of Ne spectra excited at each energy is indicated in brackets. Six lines from highly charged neon appear at 4292 Å, 4337 Å, 4378 Å, 4394 Å, 4414 Å and 4727 Å. The inverted line (dip) was caused by the background subtraction procedure, because this line (identified with carbon) was slightly more intense in the background spectra than in spectra with gas injection.

### 3.1. *Neon*

The lowest electron beam energy applied was 150 eV. This energy allows neon to be ionized to charge states up to $Ne^{6+}$ ($Ne^{5+}$ has an ionization limit of 120 eV). Because of the continuous influx of neutral neon from the gas injector, lower charge-state ions always exist in the trap, and their emissions are also recorded in the spectra. As a matter of fact, the most intense line was seen at 5856 Å and originated from neutral neon, Ne I ($2s^22p^5$ ($^2P_{1/2}$) 3s–$2s^22p^5$ ($^2P_{1/2}$) 3p) (see Fig. 3). Singly ionized neon (Ne II) emission from levels 3s, 3p, 3d and 4f was also observed. A common feature is broad asymmetrical wings in many lines that most likely represent a multitude of unresolved weak lines. One such wing was evident on the long-wavelength side of the line at 4699 Å

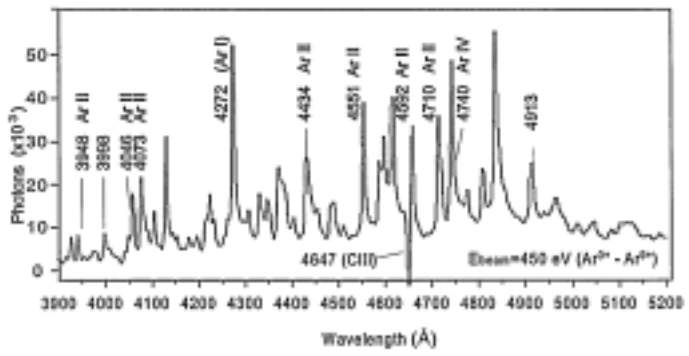


*Fig. 6.* Spectrum of argon obtained with the prism spectrograph at an electron beam energy of 450 eV. The range of spectra excited at this energy is Ar I–Ar X.

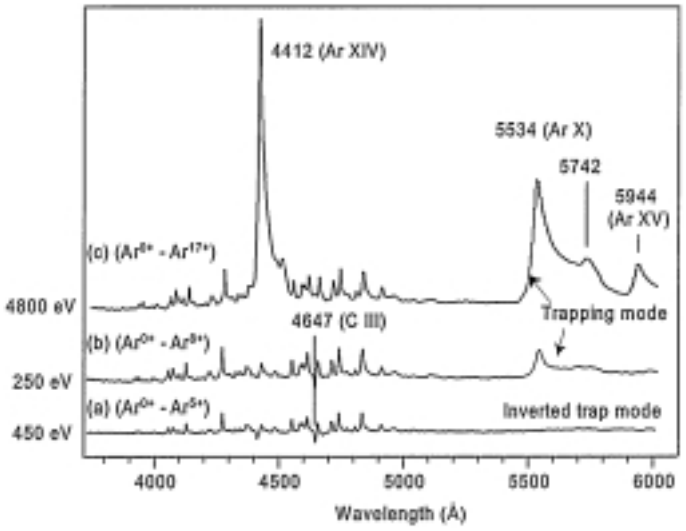


*Fig. 7.* Spectra of argon obtained with the prism spectrograph at electron energies: (a) 450 eV, (b) 250 eV and (c) 4800 eV. Spectrum (a) was recorded in the inverted-trap mode. (b) and (c) were recorded in trapping mode. The range of excited spectra is (a) Ar I–Ar VI, (b) Ar I–Ar IX, and (c) Ar I–Ar XVIII.

(see Fig. 4 and Fig. 5). Limited by the resolving power of our spectrometer, we cannot resolve most of the details of the wing. There is a weak feature at 4727 Å, which we tentatively identify to be from a magnetic dipole (M1) transition Ne IV $2s^22p^3$–$^2D_{3/2}$ $^2P_{1/2}$. However, we were not able to resolve its companion $2s^22p^3$ $^2D_{5/2}$–$^2P_{3/2}$, at 4714.25Å [22].

Fig. 4 shows neon spectra at three electron beam energies (170 eV, 250 eV, and 310 eV). The figure clearly shows the change in the relative intensities of the line features as the excitation energy is changed. Seven relatively weak lines from high ionization states can be recognized (Fig. 5). The line at 4293 Å first appears at a beam energy of 190 eV, which corresponds to Be-like Ne VII. Using the same method of threshold appearance, we tentatively identified the charge states of the other spectral lines that seem to emanate from high ionization states of Ne: Ne VII 4337 Å, 4394 Å, and 5323 Å, and Ne VIII at 4379 and 4414 Å. We were not yet able to identify the transitions that correspond to these lines, although we point out that there are beam-foil spectra that indicate optical transitions of high principal quantum number $n$ of Ne VI to Ne IX in this wavelength region [10].

We have determined the wavelengths and possible charge state of the line features for neon by using the inverted-trap technique as well as the line excitation threshold energies. We also listed possible transition identification of those lines referring to the existing database. This information is available on request to interested readers.

### 3.2. *Argon*

For the argon measurements the beam energy was varied from 150 eV to 4800 eV. Of the charge-states lower than $Ar^{8+}$, we have tentatively identified about half of the observed features, and most of these are from Ar II with the configuration $3s^23p^43l$–$3s^23p^44l'$. Figure 6 shows the argon spectrum recorded at an electron beam energy of 450 eV, with strong lines and their possible identifications marked. Similar to the measurements of the neon spectrum, the C III line at 4647 Å has been observed throughout the argon measurements, and it shows again as a feature of slightly over-subtracted intensity in the spectra at several electron energies.

Figure 7 shows argon spectra recorded at three different experimental setups. There are two spectra from ion trapping mode at two electron beam energies 250 eV, 4800 eV (Fig. 7(b) and (c)), and one spectrum, Fig. 7 (a), which was taken in the ''inverted trap mode''. Although recorded at higher electron beam energy (450 eV), the inverted-trap spectrum largely contains the same lines as the low-energy (250 eV) trapping mode spectrum.

One prominent feature of the Ar spectrum (Fig. 7) is the line at 5534 Å, known to be due to the Ar X $2s^22p^5$ $^2P_{3/2}$ $^2P_{1/2}$ M1 transition [22]. This line first appears at an electron beam energy of 200 eV, which corresponds to $Ar^{9+}$. The relative abundance of this ion reaches its peak at an electron beam energy of 450 eV, corresponding to a maximum of the relative intensity of the line. (Note that, at the same electron beam energy, this line was absent in spectrum taken in ''inverted trap mode'', Fig. 7(a)). At higher electron energies, the intensity of this line decreases again, due to the change of the charge balance. At an electron energy of 800 eV and above, a line was observed at 5944 Å which is known as the Ar XV 2s2p $^3P_1$–$^3P_2$ M1 transition [14]. Between the 5534 Å and 5944 Å lines, there are several lines that contribute to a broad feature. Limited by the resolving power of the spectrometer, only one component could be resolved, that is a line at 5742 Å. This line was observed at beam energy of at least 250 eV, and more clearly at 450 eV. Therefore, it likely originates from charge states $Ar^{8+}$ or $Ar^{9+}$. Another prominent feature of the argon spectrum is the B-like Ar XIV $2s^22p$ $^2P_{1/2}$–$^2P_{3/2}$ M1 transition at 4412 Å [27].

Similar to the neon spectrum, by using the inverted-trap technique as well as the line excitation threshold energies, we determined the possible range of ionization states of each line features for argon. This information and possible line identifications are available on request.

## 4. Summary

We have reported broad band survey spectra of neon and argon spectra in the wavelength range 3800 Å 6000 Å using a prism spectrometer on the Livermore EBIT-II device. The electron beam ion trap with its low particle density

 

and adjustable, mono-energetic electron excitation energy offers a fresh approach to the long-standing problem of spectral analysis of rare gas ions. The electron beam energies covered all possible charge states of neon and argon, from neutral to fully ionized atoms. A number of new lines from both low and high charge states were observed and their possible charge states of origin determined. However, because of the richness of the spectral lines, we were not able to resolve many of the spectral features. This survey establishes a base for further detailed spectral studies using low-density sources such as electron beam ion traps. Any further studies will require much higher spectral resolution, and also require specific theoretical calculations in order to make progress with line identifications.

## Acknowledgement

This work was performed under the auspices of the U.S. Department of Energy by the University of California Lawrence Livermore National Laboratory under contract No. W-7405-Eng-48 and supported by the Chemical Sciences, Geosciences and Biosciences Division of the Office of Basic Energy Sciences, Office of Science, U.S. Department of Energy. We acknowledge helpful discussions with E. Träbert, and thank Profs. T. Neger and L. Windholz at Graz for lending us the prism spectrograph.

## References

1. Suckewer, S. and Hinnov, E., Phys. Rev. Lett. **41**, 756 (1978).
2. Edlén, B., Physica Scripta **T8**, 5 (1983).
3. Roberts, J. R., Pittman, T. L., Sugar, J., Kaufman, V. and Rowan, W. L., Phys Rev. A **35**, 2591 (1987).
4. Denne, B., Hinnov, E., Ramette, J. and Saoutic, B., Phys. Rev. A **40**, 1488 (1989).
5. Lynch, J. P. and Kafatos, M., Astrophys. J. Suppl. Ser. **76**, 1169 (1991).
6. Keenan, F. P. *et al*., Astrophys. J. **487**, 457 (1997).
7. Persson, W., Physica Scripta **3**, 133 (1971).
8. Norlén, C., Physica Scripta **8**, 249 (1973).
9. Ishii K., *et al*. Physica Scripta T **73**, 75 (1997).
10. Lapierre, A. and Knystautas, E. J, Physica Scripta **59**, 426 (1999).
11. Beiersdorfer, P. *et al.*, in "Atomic Data Needs for X-ray Astronomy", (Eds M. A. Bautista, T. R. Kallman and A. K. Pradhan), (NASA Goddard Space Flight Center, 2000), available on-line at http://heasarc.gsfc.nasa.gov/docs/heasarc/atomic/
12. Morgan, C. A. *et al.*, Phys. Rev. Lett. **74**, 1716 (1995).
13. Serpa, F. G. *et al.*, Phys. Rev **53**, 2220 (1996).
14. Bieber, D. J., Margolis, H. S., Oxley P. K. and Silver, J. D., Physica Scripta **T73**, 64 (1997).
15. Serpa, F. G., Bell, E. W., Meyer, E. S., Gillaspy J. D. and Roberts, J. R., Phys. Rev. A **55**, 1832 (1997).
16. Crespo López-Urrutia, J. R., Beiersdorfer, P., Widmann, K. and Decaux, V., Physica Scripta T **80**, 448 (1999).
17. Utter, S. B., Beiersdorfer, P., Crespo López-Urrutia, J. R. and Träbert, E., Rev. Sci. Instrum. **70**, 288 (1999).
18. Chen, H. *et al*., Rev. Sci. Instrum. (2000). (in press).
19. Serpa, F. G., Gillaspy J. D. and Träbert, E., J. Phys. B **31**, 3345 (1998)
20. Träbert, E. *et al*., Astrophys. J. **541**, 506 (2000).
21. Träbert, E., Utter, S. B. and Beiersdorfer, P., Phys. Lett. A **272**, 86 (2000).
22. Kaufman, V. and Sugar, J., J. Phys. Chem. Ref. Data **15**, No. 1 (1986).
23. Levine, M. A., Marrs, R. E.. Henderson, J. R., Knapp, D. A. and Schneider, M. B., Physica Scripta **T22**, 157 (1988).
24. Utter, S. B., Beiersdorfer, P., Crespo López-Urrutia, J. R. and Widmann, K., Nuclear Instrum. Meth. Phys. Res. A **428**, 276 (1999).
25. Moore, C. E., U.S. National Bureau of Standards, NSRDS-NBS 3, Section 4, (1971).
26. "CRC handbook of chemistry and physics: a ready-reference book of chemical and physical data" (Editor-in-chief, David R. Lide) 68th ed. (Publisher Boca Raton, FL: CRC Press, 1987–1988, pp. E-201–E-327.
27. "NIST Atomic Spectra Database", Web-based Version 2.0, http://physics.nist.gov (2000).

 